

Cellulose Nanocrystal Reinforced Epoxy Vinyl Ester Resins: Fabrication and Mechanical Properties

L. Thompson, M. Nikzad*, I. Sbarski, J. Miller and A. Yu

Faculty of Science, Engineering and Technology; Swinburne University of Technology, Melbourne, Australia

Abstract

Cellulose nanocrystals (CNC) were surface modified with (3-aminopropyl)triethoxysilane (APTES) to convert their native hydrophilic nature into hydrophobic. This Functionalization was found to be effective in improving the dispersion of CNC within the epoxy vinyl ester resin network. The addition of functionalised CNC enhanced mechanical properties of the vinyl ester based nanocomposites. Nanoscale dispersion of the CNC particles was proved to be a key factor in maximising mechanical properties of the matrix and keeping the nanofiller content to an optimal minimum. Tensile strength and modulus of the matrix was found to have peaked around 1-1.5% w/v loading of the CNC whereas higher loading had negative impact on the properties due to agglomeration of the nanoparticles and formation of micro inclusions. Dynamic mechanical analysis showed an approximate 1 GPa rise in the storage modulus of the CNC reinforced vinyl ester matrix compared to the neat resin. Loss modulus of the matrix of the rubbery phase beyond 100 °C remained unaffected indicating little impact on the complex viscosity of the resultant composite at lower loading of CNC. APTES based surface treatment of CNC particles was proved to be a promising route to enhance the dispersion of CNC as reinforcing fillers in vinyl ester based composite structures which have a variety of industrial applications.

Keywords

Cellulose nanocrystals, polymer nanocomposites, surface modification

1. Introduction

Cellulose has obtained a global interest in various industries including textiles, papers and as an additive in foods. Part of this can be attributed to cellulose being the most readily abundant biopolymer. This availability is enhanced by the fact that the primary sources of cellulose are plant materials, meaning that it is renewable and green. The cellulose polymer is comprised of a repeating unit of two glucoses in a β 1-4 orientation known as cellobiose, the length of this repeating unit varies depending on the individual source material used with n reaching as high as 15,000 units. Cellulose fibres are comprised of two separate parts, the more organised (crystalline) and disorganised (amorphous) regions. (Habibi et al., 2010, Moon et al., 2011)

Nanocrystalline cellulose is primarily obtained via hydrolysis; either through acids (Oksman et al., 2006, Junior de Menezes et al., 2009, Pasquini et al., 2010, Chen et al., 2015, Li et al., 2015, Dong et al., 2016, Guo et al., 2016) or enzymes (Pääkkö et al., 2007). The treatment leads to the removal of amorphous regions, leaving only the crystalline parts. Typically, the hydrolysis method is performed using concentrated sulphuric acid (varying around 50 to 70 wt%) (Chen et al., 2015, Dong et al., 2016). The sulphuric acid treatment has the added benefit of creating a negative charge on the surface of the remaining crystalline regions. The remaining crystalline cellulose can be further broken down by the application of mechanical energy. The process involves the shearing of the cellulose fibrils cleaving across an axis, creating long singular chains which are then reduced via repeated processing, breaking down into individual nanowhiskers (Braun and Dorgan, 2009, Junior de Menezes et al., 2009, Csiszar et al., 2016). Mechanical processing is somewhat limited due to the creation of hydrogen bonds between the individual nanocrystals forming large agglomerates.

The production of nanocellulose has been an area of interest in recent years due to multiple positive properties such as high aspect ratio, low density, high affinity to water, high tensile modulus and easy modification due to hydroxyl groups present (Moon et al., 2011). Due to these positive properties cellulose nanocrystals have gained interest in the use as a nanofiller in polymer networks.

A controlled dispersion of CNC in a thermoset resin matrix has the commercial attractiveness of enabling a low cost boost to the performance for structural composite applications. Specific benefits such as improved thermal stability, increased stiffness and resilience as well as the potential to reduce the volume of material and hence reduce mass, are highly valued properties in composite components used for transport applications. Developments in low cost

nanocomposites have the potential to open the floodgates to a mainstream market for the replacement of medium to high strength steels in chassis and other structural parts in automotive applications and may also bridge the performance gap in some high end aerospace applications where carbon fibre reinforced composites are typically used. Other possible applications include wind turbine blades and marine craft structures.

The addition of the nanocrystals has been explored in various different polymers including polyvinyl alcohol (Mbhele et al., 2003, Roohani et al., 2008, Liang et al., 2009), polyethylene (Goetz et al., 2009, Junior de Menezes et al., 2009), polyurethane (Petrović et al., 2000, Cao et al., 2007, Girouard et al., 2016), unsaturated polyester resin (Kargarzadeh et al., 2015a, Kargarzadeh et al., 2015c), poly(lactic acid) (Oksman et al., 2006), chitosan (Celebi and Kurt, 2015), epoxy resin (Girouard et al., 2015, Khelifa et al., 2016, Ma et al., 2016) and rubber (Pasquini et al., 2010).

It has been some reports on the incorporation of CNC into polymer network to improve the properties of nanocomposites. For example, previous work has explored the use of CNC in water based epoxies (Xu et al., 2013, Girouard et al., 2015) showing that it was a successful method for improving the intended properties. It has also been shown that the addition of pure CNC to an organic based resin does lead to some improvement however it is very limited to low volume fractions of the filler due to the formation of agglomerates. Till now, the direct use of CNC has been rather limited due to its highly hydrophilic nature which makes difficult to be dispersed within anything that isn't water based.

For CNC to be properly incorporated into an organic system it requires surface modification to reduce the hydrophilic properties. This functionalization is typically done by removing/replacing the hydroxyl groups which are present on the surface of the CNC. Research has previously explored various pathways of modifying CNC to improve the dispersion, these pathways include TEMPO oxidation (Montanari et al., 2005, Li et al., 2015, Sun et al., 2015), use of surfactants (Heux et al., 2000), polymer grafting (Junior de Menezes et al., 2009), isocyanates (Siqueira et al., 2010, Girouard et al., 2016) and as was also looked at in this paper the use of silane coupling agents (de Oliveira Taipina et al., 2013, Kargarzadeh et al., 2015a, Kargarzadeh et al., 2015c).

In this work, the use of a silane coupling agent ((3-aminopropyl)triethoxysilane) was decided as it was hoped to use a one pot method of production allowing for a simple modification

process which could potentially be scaled up to levels of productions that would be found in industry.

2. Materials and Methods

2.1 Materials

(3-aminopropyl)triethoxysilane (APTES, 95%), methyl methacrylate (MMA), absolute ethanol and acetic acid (99%) were obtained from Sigma Aldrich. Vinyl ester resin and initiator methyl ethyl ketone peroxide composition (Norox MEKP-H925) were obtained from Nuplex Composites, Australia. Cellulose nanocrystals (CNC) were donated by the United States Department of Agriculture's Forest Products Laboratory in association with the Cooperative Research Centre for Advanced Automotive Technologies and the Australian based automotive interiors manufacturer.

2.2 Functionalization of CNC

CNC functionalization was performed using a modified method from Kargarzadeh et al (Kargarzadeh et al., 2015c). CNC was dispersed into an ethanol solution containing 2% v/v APTES which then had its pH reduced to be approximately 4 using acetic acid. The solution was sonicated for 15 minutes and left to rest for 3 hours at room temperature. The resulting modified CNC was collected via centrifugation followed by washing with absolute ethanol to remove any excess silane. The APTES modified CNC was then dried in oven for future usage.

2.3 Production of Vinyl Ester Resin/CNC hybrids

The desired amount of the APTES modified CNC was mixed into 10 mL MMA. After sonication for 10 minutes, the CNC/MMA solution was added into 90 mL vinyl ester resin. The mixture was sonicated in an ice bath for 30 minutes with some stirring.

The resin then had 1.25% MEKP-H 925 added into it under vigorous stirring. The mixture was left to rest for 10 minutes to remove any bubbles that were produced. Any additional bubbles that remained on the surface were popped by grouping them to the edge of the container used using a glass rod.

After settling the resin was poured into mould and placed in the oven to cure at 80 °C for 5 hours. After cooling to room temperature, samples were buffed with 120 and then 480 grain sand papers using an orbital sander at 400 RPM.

Thick film samples with an approximate thickness of 2 mm for dynamic mechanical thermal analysis (DMA) were also produced by mixing 14.4 mL of the resin with 1.6 mL of the mixed solution of MMA and APTES/CNC. After sonication the resin had the same process for activation and was poured into petri dishes and left to cure for 2 hours at room temperature. Samples were then removed from dishes and cured in the oven for 5 hours at 80 °C.

The produced thick films were then buffed to obtain a consistent width and were then cut to size of approximately 35 by 12 mm.

2.4 Characterisation

2.4.1 Fourier Transfer Infra-Red Spectroscopy

Fourier Transfer Infra-Red Spectroscopy (FTIR) was carried out to explore whether the APTES was successfully grafted to the CNC. It was performed using a Thermo Scientific Nicolet iS5 FT-IR Spectrometer, with 10 scans being performed per test.

2.4.2 Zeta Potential

Zeta Potential and particle sizing of CNC and APTES/CNC were measured in water, ethanol and MMA, these different solvents were selected based on their polarity. MMA was primarily selected as an organic solvent due to its common use in polymers as an additive.

To explore the stability of the dispersion, 0.1 g APTES/CNC was placed into approximately 2.5 mL of each solvent. It was then sonicated for 30 minutes before being left to sit for two days to look at how well the particles would stay dispersed within the solution.

2.4.3 Tensile Tests

Tensile tests of the produced resin samples were performed on a Zwick Z010 universal testing machine. According to American Society for Testing and Materials standard (ASTM D638), the test speed and gauge length were set at 5 mm/min and 100 mm respectively. Small test speed was used due to brittleness of the thermoset samples. A minimum number of 5 test specimens were used to check for the reproducibility of the results.

2.4.4 Scanning Electron Microscopy

Surface morphology of produced resin hybrids was inspected using a ZEISS Supra 40VP Scanning Electron Microscope (SEM). SEM scans were performed on cross sections of resin samples which had been broken during the tensile tests. Prior to scanning, samples were coated with a thin layer of gold to improve the conductivity.

2.4.5 Transmission Electron Microscopy

TEM was performed to examine the dispersion of the APTES/CNC at the nanoscale within the resin. Samples were first cut into 1 cm x 3 cm pieces and washed with copious amount of nanopure H₂O (with a resistivity of 18.2 MW cm⁻¹), dried with 99.99% purity nitrogen gas. These pieces were then trimmed, cut into ultrathin sections (80 nm thickness) using a Leica EM UC7 ultramicrotome (Leica Microsystems, Wetzlar, Germany) with a diamond knife (Diatome, Pennsylvania, USA). Sections were placed onto 300 mesh copper grids and examined using a JEM 1010 instrument (JEOL, Frenchs Forest, Australia). Approximately 15 TEM images taken at ×10000 and ×20000 magnifications for each sample were analysed.

2.4.6 Dynamic Mechanical Thermal Analysis

DMA was performed on the produced thick films on a 2980 DMA machine from TA Instruments. The parameters were set to be 35 °C for the starting temperature increasing at a rate of 5 °C per minute to a maximum of 150 °C. The test performed was a single cantilever test with a gap width of 17.5 mm on pieces of thick film with dimensions being roughly 12 mm wide and 35 mm long.

2.4.7 Thermogravimetric Analysis

TGA was performed on an SDT 2960 Simultaneous DSC-TGA from TA Instruments. Approximately 5 mg of each sample was used to perform the test; the starting temperature was set to be 50 °C increasing with a rate of 10 °C per minute to a maximum of 500 °C using air as the gas.

3. Results and Discussion

3.1 Functionalization of CNC with APTES

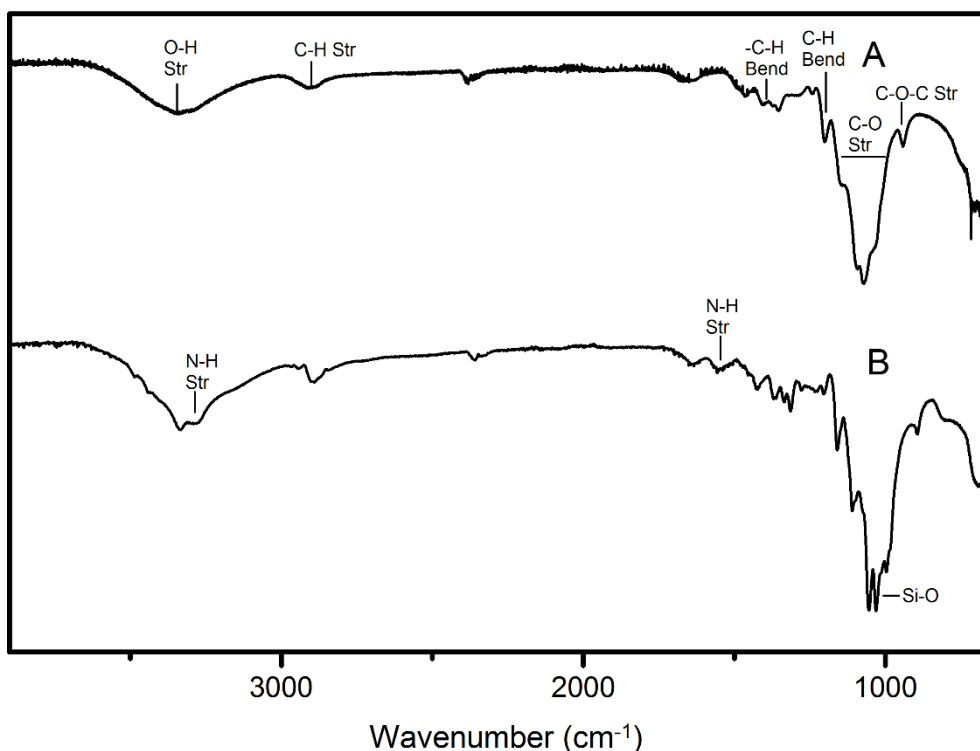


Figure 1: FTIR spectra of (A) CNC and (B) APTES modified CNC.

After being modified with APTES, there was a noticeable colour change of CNC, turning from white to a light brown. FTIR spectra (*Figure 1*) further confirmed that the functionalization has occurred. Compared to the spectrum of unmodified CNC (curve A), additional peaks appear after reaction with APTES (curve B). The new peak around 1100 cm^{-1} can be attributed to the Si-O bonding formed between APTES and the hydroxyl groups of CNC. Additional peak of amino groups from APTES could be seen at approximate 1600 cm^{-1} . At 1300 cm^{-1} the Si-C bonding from APTES can be found as well. These peaks confirm that APTES has been successfully grafted onto CNC. It is noticed that there is still a distinct peak around 3400 cm^{-1} that is related to the hydroxyl group of CNC. This indicates that there are still some hydroxyl groups unreacted after APTES modification.

Visually alone there was a noticeable difference in dispersibility between the modified and unmodified CNC. As can be seen in *Figure 2*, the unmodified CNC forms a stable and uniform dispersion in water due to the abundant hydroxyl groups on surface. Because some hydroxyl groups still remain after APTES modification (see above FTIR results), the APTES/CNC is also able to form a water dispersion. However, the dispersion is not stable and APTES/CNC settles very quickly to the bottom of the centrifuge tube. This result further supports the successful functionalization of APTES on CNC. When comparing the dispersion in other two

organic solvents including ethanol and MMA, the APTES modified CNC performed much better in forming stable dispersions. This is especially noticeable within MMA where there was no visible agglomeration (*Figure 2F*).

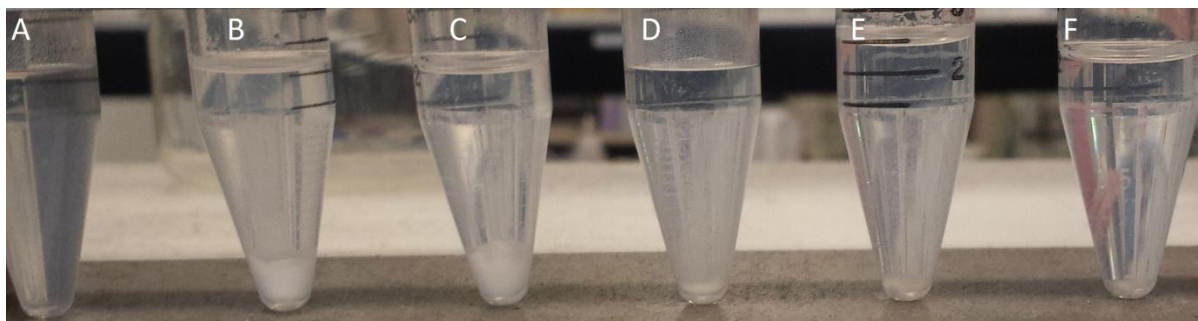


Figure 2: Images of CNC and APTES/CNC dispersed in different solvents. CNC in (A) water, (B) ethanol, (C) MMA, and APTES/CNC in (D) water, (E) ethanol and (F) MMA.

Table 1: Zeta Potentials of CNC and APTES/CNC in different solvents.

Zeta Potential (mV)	H ₂ O	Ethanol	MMA
CNC	-39.5	-30.2	-0.5
APTES/CNC	-13.3	-14.3	-3.9

Table 1 shows the Zeta potentials of CNC and APTRES/CNC measured in three different solvents. CNC have a very high negative zeta potential (-39 mV) in water, again due to the hydroxyl groups on surface. This also explains its excellent dispersibility in water. The zeta potential of APTES/CNC in water is -13.3 mV which is much lower than CNC in comparison, showing that there had been a reduction in the number of hydroxyl groups on surface. Similar results were found in ethanol; this isn't too surprising as ethanol is still a rather polar solvent. However, the zeta potential in MMA gives a different result, with the APTES/CNC having a more negative value. This might explain the better dispersity of APTES/CNC in MMA. However, further tests may be needed to confirm the exact Zeta potentials in MMA as it partially polymerised during testing, which could impact its zeta potential reading.

Table 2: Particle size of CNC and APTES/CNC measured in different solvents.

Particle Size (nm)	H ₂ O	Ethanol	MMA
CNC	14	679	79

APTES/CNC	3044	513	130
-----------	------	-----	-----

Table 2 shows the particle size of CNC and APTES/CNC measured in the same three solvents. In water the particle size for the CNC was about 14.4 nm which is within the range provided by the company. The true size of CNC particles would be difficult to accurately obtain from particle sizing due to their more rod-like structure. Compared to CNC, the APTES/CNC sample had a much larger particle size in water which was now measured in the microscale. The result would be due to the reduced surface charge leading to large agglomerates. The particle size of CNC in ethanol increased significantly, which relates to the reduction in the zeta potential and the creation of agglomerates between the individual particles. The fact that the sizes of APTRES/CNC in ethanol and MMA were much less than it in water indicates that the surface modification of APTRES greatly improves the dispersibility of CNC in organic solvents such as MMA.

From both tests there was found to be a change after functionalization, indicating that it had been successful in reducing the hydrophilic nature of cellulose. The reduction however was not perfect as there were still some hydroxyl groups present. This result was backed by the FTIR which shows the remaining presence of some hydroxyl groups which are believed cause for the overall hydrophilicity of CNC.

4.2 Resin/CNC composite materials

4.2.1 Preparation of Resin/CNC films

During the production of resin samples, it was noticed that the colour of the resin would change as the concentration of the APTES/CNC increased in the sample. Starting as an orange colour, over time would become darker eventually becoming closer to brown. This was an indication of the difference between the produced samples as the loading ratios were altered.

It was proposed that this colour change was due to the interactions between the amine group of APTES with metal ions present within the resin. This could be an issue as it is unclear if this interaction did happen and what effects it had on the curing process of the resin used.

The samples were cured in a regular oven due to worries that the process being performed in a vacuum oven would lead to further increases of the inherent stress within the produced resins.

4.2.2 Morphology of Resin/CNC films

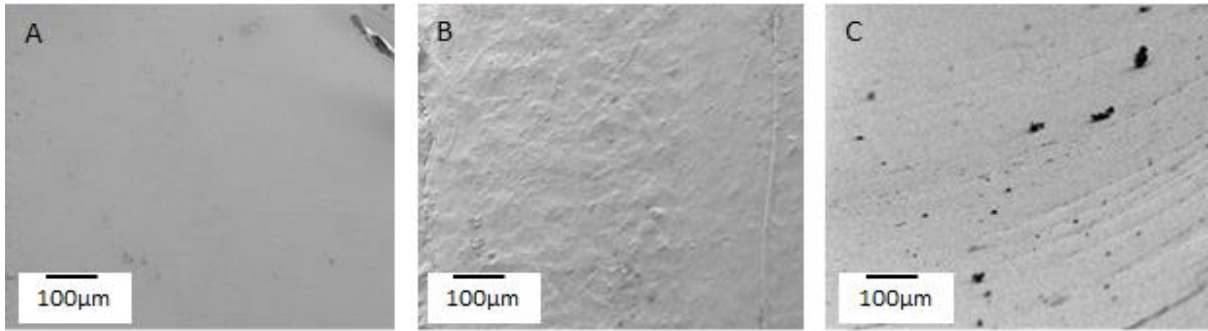


Figure 3: Cross-section SEM images of the composites with varying loading of the APTES/CNC in VER. (A) Blank Resin, B 0.1% APTES/CNC and C 1% APTES/CNC.

Figure 3 shows the cross-section SEM images of the blank resin and resin composites with 0.1% and 1% APTES/CNC loading. There was noticeable difference in surface feature as the concentration of CNC increased. The surface roughness of the resin also appeared to increase showing more signs of imperfections. This can be explained by the APTES/CNC taking up parts within the polymer network disrupting the overall packing of the polymer.

From the SEM results it was difficult to confirm whether or not the modified CNC was properly distributed throughout the resin network. TEM was then used to confirm the incorporation of CNC into the resin network. As can be seen in *Figure 4*, there was poor distribution of CNC within the epoxy vinyl ester with large agglomerates being formed. The diameter of particles ranged from being greater than 200 nm down to under 50 nm.

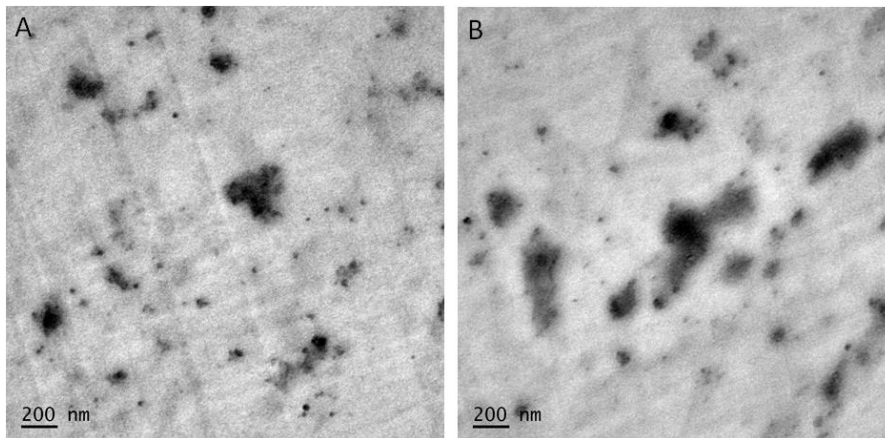


Figure 4: TEM images of produced plastics with (A) 0.5% and (B) 1% APTES/CNC loading.

Thus the concentration increase of CNC could induce the agglomerates of CNC particles. These agglomerates could be potentially points of weakness within the formed plastics, leading to premature breaking of samples when testing the mechanical properties. The un-uniform

distribution helps explain the variation within individual results (see below), as the concentration would be different depending on the tested area for the produced samples.

4.2.3 Mechanical Properties

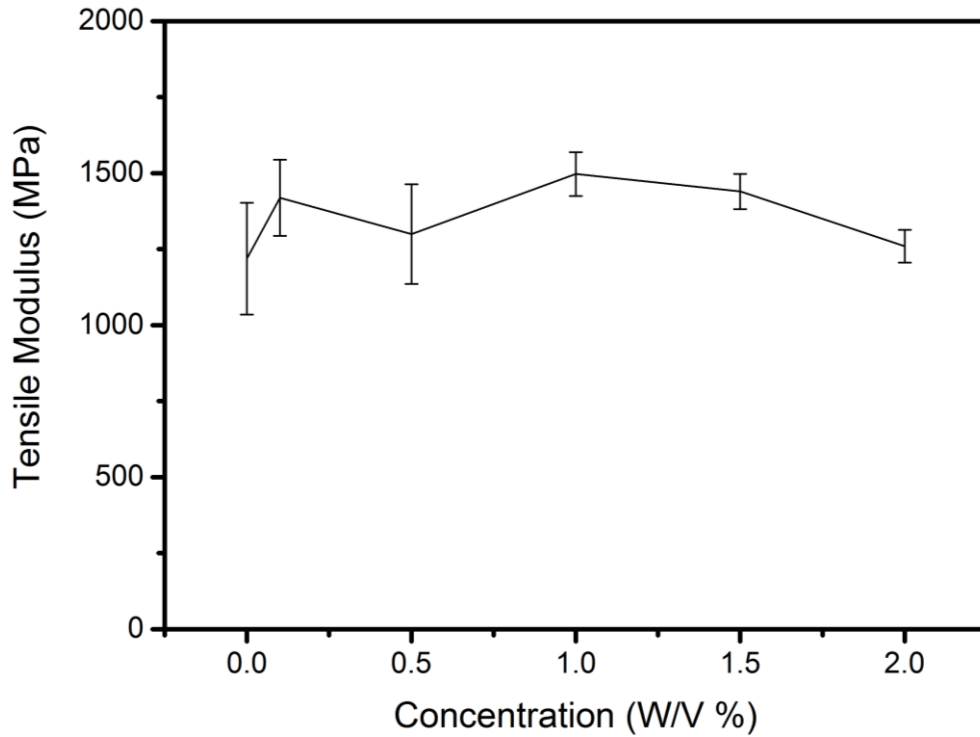


Figure 5: Tensile modulus of composites with different loading precents of APTES/CNC.

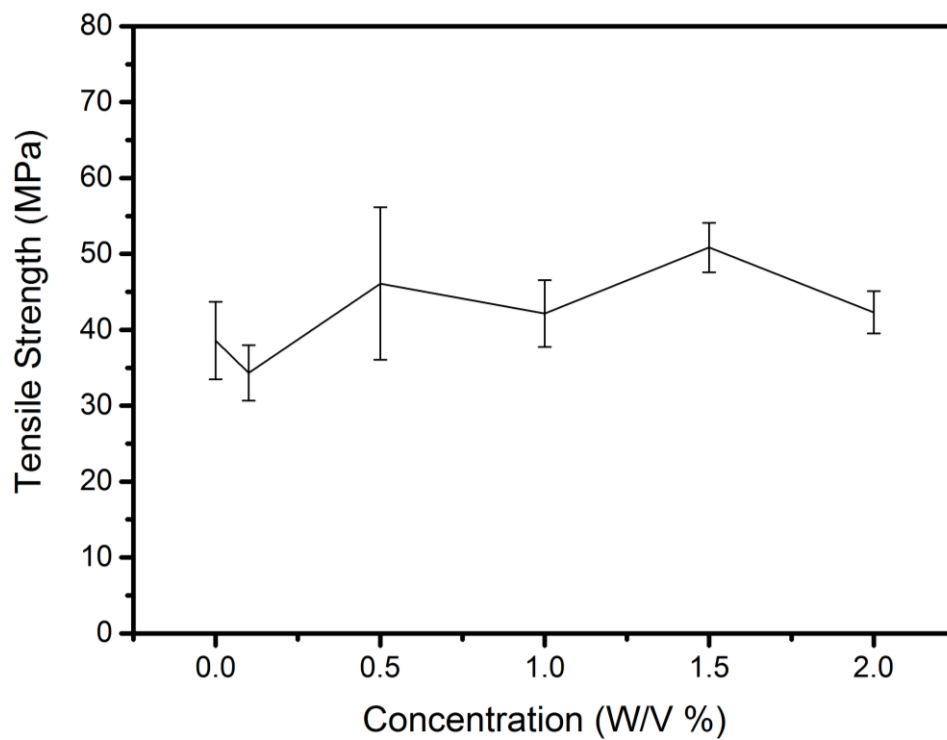


Figure 6: Tensile strength of the resin composites with different loading of APTES/CNC.

Figure 5 and 6 represent the tensile strength and modulus for the resin composites with different loading of APTES/CNC. The data show a rather inconsistent trend where it would increase overall until eventually decreasing. The problem with this arises from the fact that there was the opposite occurring; where an increase from the previous in the modulus was met by a decrease in the tensile strength. The only sample that this problem does not occur is the composite with 2% loading where both tensile strength and modulus had a decrease, suggesting that it was beyond the limit for effective loading.

It is difficult to say whether this trend is consistent due to the substantial error found within these tests, especially for the modulus. With the blank resin having a variation significant enough to cover at least part of the variation in nearly each sample that was tested. As the disparity was so significant, it cannot be confirmed how much of the improvement was from the addition of the APTES/CNC instead of just being the blank resin.

However, when considering the error, it can be found that there is not that great an improvement in the tensile modulus. The greatest improvement compared to the base resin was still under 300 MPa difference and is roughly a 18% improvement overall. It is very likely that the obtained maximum tensile strength is not the true maximum due to the break down.

The tensile strength had a more noticeable improvement than the modulus; it was found to have a maximum that was about 31% better than the base resin. The variation within the tensile strength was also much lower in comparison to the modulus.

4.2.4 Thermal Properties

DMA was performed to explore the stress/strain and rheological properties of the plastics produced. From the DMA graph in *Figure 7*, it was found that compared to the base resin there was an improvement in the storage modulus. Even with the lowest loading of 0.1% it still had close to a 0.7 GPa increase for the maximum value. There was a general increase in the storage modulus up to 1.5% loading after which there was a decrease. The sample with 2% loading has the similar modulus to that of the 0.1% sample.

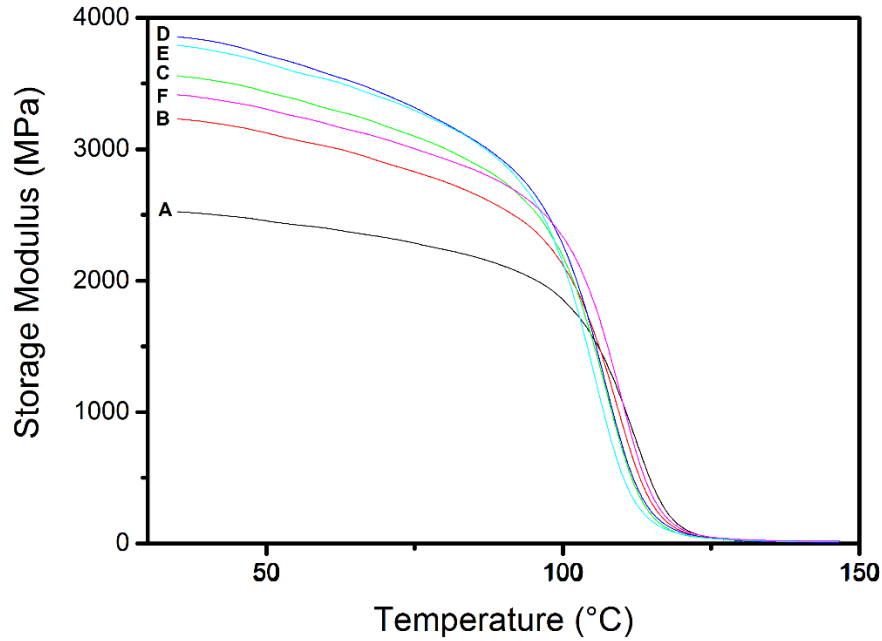


Figure 7: DMA graphs of composites with different APTES/CNC loadings. A: Vinyl ester resin only, B: 0.1 % APTES/CNC, C: 0.5% APTES/CNC, D: 1% APTES/CNC, E: 1.5% APTES/CNC and F 2% APTES/CNC.

All the tested samples appeared to have a drop at around the same temperature (about 110 °C) without much significant variation between these results. This showed there was little effect on the point at which mechanical failure begins; implying that there was not a great effect on the thermal stability and glass transition from the addition of the APTES/CNC. However, it is worth noting that samples with 1 and 1.5 % loading (which had the highest storage modulus) also had the earliest onset for the mechanical failure. But this onset is still a rather negligible difference in comparison.

It was proposed that part of the limitation leading to a decrease in the storage modulus at such a low loading was due to the presence of amine groups from APTES. These amine groups could interact with metal ions present in the VER which inhibit the initiation of the curing process.

From the Tan Delta Peak shown in *Figure 8*, it was found that there was a reduction in the temperature required for the resin used to obtain its glass transition. The Tan Delta gives a much clearer indication of the glass transition compared to the storage modulus. There was a notable decrease in the storage modulus from the start of the experiment until it reached what was approximately the beginning of the glass transition. Some of this alteration could be

explained by the addition of the nanofiller leading to a less cohesive crosslinking occurring within the resin network.

What is interesting to note is that the movement of the peak is related to the storage modulus as the 2% loading had a higher value compared to the two previous samples which suggests that the addition of the CNC was not the direct effect causing the reduction.

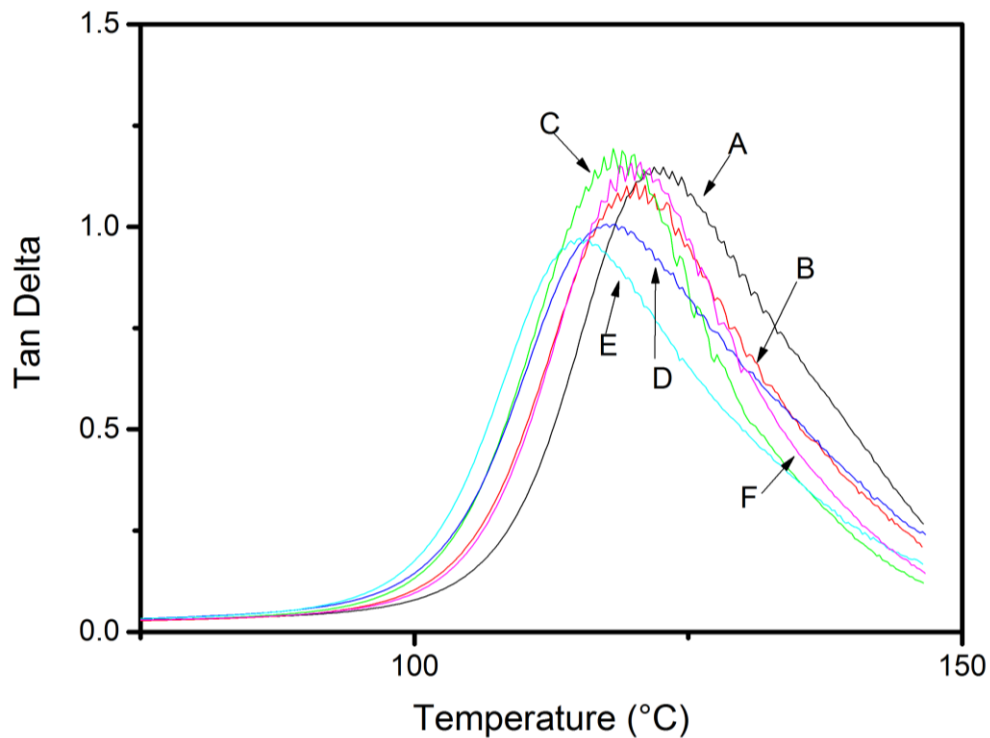


Figure 8: Comparison of Tan Delta information for produced resin samples. A: Vinyl ester resin only, B: 0.1 % APTES/CNC, C: 0.5% APTES/CNC, D: 1% APTES/CNC, E: 1.5% APTES/CNC and F 2% APTES/CNC.

Figure 9 represents the TGA graph of the resin composites. There was little difference between individual samples. CNC would burn at about approximately 300 °C which can be seen in the insert of *Figure 9* where there is a small drop in the percentage. However, this difference is not very discernible in comparison to the blank vinyl ester resin. This small distinction would also be due to the fact that the samples had such a small loading of the APTES/CNC. This would be at best a 2% difference in weight which is rather negligible in the total graph.

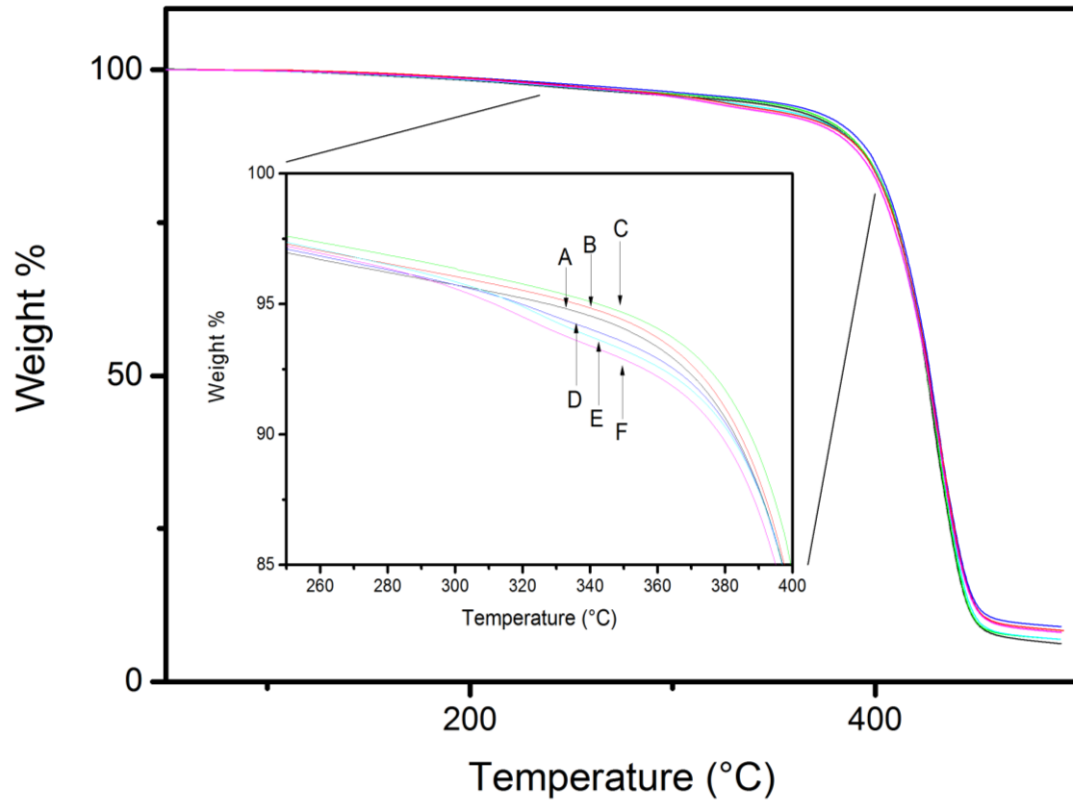


Figure 9: Combination of results obtained from the TGA. A: Vinyl ester resin only, B: 0.1 % APTES/CNC, C: 0.5% APTES/CNC, D: 1% APTES/CNC, E: 1.5% APTES/CNC and F 2% APTES/CNC.

Since there were no serious changes within the TGA results, it can be concluded that the addition of the APTES/CNC did not have a significant impact upon the thermal stability of the resin used.

4. Conclusion

The modification of CNC by APTES was found to successfully reduce its hydrophilic surface nature. The modification was confirmed by FTIR which showed additional peaks were added to the CNC similar to the ones expected from the APTES. Further evidence of modification can be seen in the changes in Zeta potential and particle size. Especially in water, the zeta potential APTES/CNC was decreased greatly due to the reduction in surface charge, and the particle sizing were far larger due to the formation agglomerates in water.

The addition of the APTES modified CNC into the epoxy vinyl ester was found to lead to an improvement in the mechanical properties. Both the tensile strength and modulus were

improved even with a 0.1% loading. The maximum possible loading was found to be around 1.5%, above which a decrease was found in comparison to the blank sample. The tensile testing was rather limited due to the individual variation during the production of the sample. The DMA results indicated that there was a significant improvement to the storage modulus, with both samples of 1 and 1.5% loading reaching close to a 1 GPA increase over the blank. There was no significant difference in the loss modulus indicating that the thermal stability was not greatly impacted by the further addition of CNC.

From the mechanical data it could be argued that 1% loading was the preferred option as negligible difference was found between samples of 1% and 1.5% loading. Because 1% loading only requires two thirds of CNC, it has the advantage on larger scale production.

Whilst modification with APTES was successful, the current method still has the limitation due to the formation of CNC agglomerates. These agglomerates prevent the uniform distribution of CNC within the polymer network to form a desirable nanocomposite material. Further studies on the improvement of the dispersibility of CNC in resin are currently underway in our lab.

Acknowledgement:

Authors would like to thank Mr Peter Nguyen for his assistance in obtaining TEM images of the samples. The support of Commonwealth Research Centre for Automotive, Australia in obtaining CNC materials from UFPL is also greatly appreciated.

References

- BRAUN, B. & DORGAN, J. R. 2009. Single-step method for the isolation and surface functionalization of cellulosic nanowhiskers. *Biomacromolecules*, 10, 334-341.
- CAO, X., DONG, H. & LI, C. M. 2007. New Nanocomposite Materials Reinforced with Flax Cellulose Nanocrystals in Waterborne Polyurethane. *Biomacromolecules*, 8, 899-904.
- CELEBI, H. & KURT, A. 2015. Effects of processing on the properties of chitosan/cellulose nanocrystal films. *Carbohydrate Polymers*, 133, 284-293.
- CHEN, L., WANG, Q., HIRTH, K., BAEZ, C., AGARWAL, U. P. & ZHU, J. Y. 2015. Tailoring the yield and characteristics of wood cellulose nanocrystals (CNC) using concentrated acid hydrolysis. *Cellulose*, 22, 1753-1762.
- CSISZAR, E., KALIC, P., KOBOL, A. & FERREIRA, E. D. P. 2016. The effect of low frequency ultrasound on the production and properties of nanocrystalline cellulose suspensions and films. *Ultrasonics Sonochemistry*, 31, 473-480.

- DE OLIVEIRA TAIPINA, M., FERRAREZI, M. M. F., YOSHIDA, I. V. P. & GONÇALVES, M. C. 2013. Surface modification of cotton nanocrystals with a silane agent. *Cellulose*, 20, 217-226.
- DONG, S., BORTNER, M. J. & ROMAN, M. 2016. Analysis of the sulfuric acid hydrolysis of wood pulp for cellulose nanocrystal production: A central composite design study. *Industrial Crops and Products*.
- GIROUARD, N., SCHUENEMAN, G. T., SHOFNER, M. L. & MEREDITH, J. C. 2015. Exploiting colloidal interfaces to increase dispersion, performance, and pot-life in cellulose nanocrystal/waterborne epoxy composites. *Polymer (United Kingdom)*, 68, 111-121.
- GIROUARD, N. M., XU, S., SCHUENEMAN, G. T., SHOFNER, M. L. & MEREDITH, J. C. 2016. Site-Selective Modification of Cellulose Nanocrystals with Isophorone Diisocyanate and Formation of Polyurethane-CNC Composites. *ACS Applied Materials and Interfaces*, 8, 1458-1467.
- GOETZ, L., MATHEW, A., OKSMAN, K., GATENHOLM, P. & RAGAUSKAS, A. J. 2009. A novel nanocomposite film prepared from crosslinked cellulosic whiskers. *Carbohydrate Polymers*, 75, 85-89.
- GUO, J., GUO, X., WANG, S. & YIN, Y. 2016. Effects of ultrasonic treatment during acid hydrolysis on the yield, particle size and structure of cellulose nanocrystals. *Carbohydrate Polymers*, 135, 248-255.
- HABIBI, Y., LUCIA, L. A. & ROJAS, O. J. 2010. Cellulose Nanocrystals: Chemistry, Self-Assembly, and Applications. *Chemical Reviews*, 110, 3479-3500.
- HEUX, L., CHAUVE, G. & BONINI, C. 2000. Nonflocculating and Chiral-Nematic Self-ordering of Cellulose Microcrystals Suspensions in Nonpolar Solvents. *Langmuir*, 16, 8210-8212.
- JUNIOR DE MENEZES, A., SIQUEIRA, G., CURVELO, A. A. S. & DUFRESNE, A. 2009. Extrusion and characterization of functionalized cellulose whiskers reinforced polyethylene nanocomposites. *Polymer*, 50, 4552-4563.
- KARGARZADEH, H., SHELTAMI, R. M., AHMAD, I., ABDULLAH, I. & DUFRESNE, A. 2015a. Cellulose nanocrystal reinforced liquid natural rubber toughened unsaturated polyester: Effects of filler content and surface treatment on its morphological, thermal, mechanical, and viscoelastic properties. *Polymer (United Kingdom)*, 71, 51-59.
- KARGARZADEH, H., SHELTAMI, R. M., AHMAD, I., ABDULLAH, I. & DUFRESNE, A. 2015c. Cellulose nanocrystal: A promising toughening agent for unsaturated polyester nanocomposite. *Polymer (United Kingdom)*, 56, 346-357.
- KHELIFA, F., HABIBI, Y., BONNAUD, L. & DUBOIS, P. 2016. Epoxy Monomers Cured by High Cellulosic Nanocrystal Loading. *ACS Applied Materials and Interfaces*, 8, 10535-10544.
- LI, B., XU, W., KRONLUND, D., MÄÄTTÄNEN, A., LIU, J., SMÅTT, J. H., PELTONEN, J., WILLFÖR, S., MU, X. & XU, C. 2015. Cellulose nanocrystals prepared via formic acid hydrolysis followed by TEMPO-mediated oxidation. *Carbohydrate Polymers*, 133, 605-612.
- LIANG, J., HUANG, Y., ZHANG, L., WANG, Y., MA, Y., CUO, T. & CHEN, Y. 2009. Molecular-level dispersion of graphene into poly(vinyl alcohol) and effective reinforcement of their nanocomposites. *Advanced Functional Materials*, 19, 2297-2302.
- MA, H., HU, N., WU, C., ZHU, Y., CAO, Y. & CHEN, Q. Q. 2016. Synthesis and research of epoxy resin toughening agent. *SpringerPlus*, 5, 1-10.
- MBHELE, Z. H., SALEMANE, M. G., VAN SITTERT, C. G. C. E., NEDELJKOVIĆ, J. M., DJOKOVIĆ, V. & LUYT, A. S. 2003. Fabrication and Characterization of Silver-Polyvinyl Alcohol Nanocomposites. *Chemistry of Materials*, 15, 5019-5024.

- MONTANARI, S., ROUMANI, M., HEUX, L. & VIGNON, M. R. 2005. Topochemistry of carboxylated cellulose nanocrystals resulting from TEMPO-mediated oxidation. *Macromolecules*, 38, 1665-1671.
- MOON, R. J., MARTINI, A., NAIRN, J., SIMONSEN, J. & YOUNGBLOOD, J. 2011. Cellulose nanomaterials review: structure, properties and nanocomposites. *Chemical Society Reviews*, 40, 3941-3994.
- OKSMAN, K., MATHEW, A. P., BONDESON, D. & KVIEN, I. 2006. Manufacturing process of cellulose whiskers/polylactic acid nanocomposites. *Composites Science and Technology*, 66, 2776-2784.
- PÄÄKKÖ, M., ANKERFORS, M., KOSONEN, H., NYKÄNEN, A., AHOLA, S., ÖSTERBERG, M., RUOKOLAINEN, J., LAINE, J., LARSSON, P. T., IKKALA, O. & LINDSTRÖM, T. 2007. Enzymatic Hydrolysis Combined with Mechanical Shearing and High-Pressure Homogenization for Nanoscale Cellulose Fibrils and Strong Gels. *Biomacromolecules*, 8, 1934-1941.
- PASQUINI, D., TEIXEIRA, E. D. M., CURVELO, A. A. D. S., BELGACEM, M. N. & DUFRESNE, A. 2010. Extraction of cellulose whiskers from cassava bagasse and their applications as reinforcing agent in natural rubber. *Industrial Crops and Products*, 32, 486-490.
- PETROVIĆ, Z. S., JAVNI, I., WADDON, A. & BÁNHEGYI, G. 2000. Structure and properties of polyurethane-silica nanocomposites. *Journal of Applied Polymer Science*, 76, 133-151.
- ROOHANI, M., HABIBI, Y., BELGACEM, N. M., EBRAHIM, G., KARIMI, A. N. & DUFRESNE, A. 2008. Cellulose whiskers reinforced polyvinyl alcohol copolymers nanocomposites. *European Polymer Journal*, 44, 2489-2498.
- SIQUEIRA, G., BRAS, J. & DUFRESNE, A. 2010. New Process of Chemical Grafting of Cellulose Nanoparticles with a Long Chain Isocyanate. *Langmuir*, 26, 402-411.
- SUN, X., WU, Q., REN, S. & LEI, T. 2015. Comparison of highly transparent all-cellulose nanopaper prepared using sulfuric acid and TEMPO-mediated oxidation methods. *Cellulose*, 22, 1123-1133.
- XU, S., GIROUARD, N., SCHUENEMAN, G., SHOFNER, M. L. & MEREDITH, J. C. 2013. Mechanical and thermal properties of waterborne epoxy composites containing cellulose nanocrystals. *Polymer (United Kingdom)*, 54, 6589-6598.